Secretory Ameloblasts and Calcium Distribution During Normal and Experimentally Altered Mineralization

S. H. Ashrafi
College of Dentistry

Dale R. Eisenmann
College of Dentistry

A. E. Zaki
College of Dentistry

Utah State University
MERRILL-CAZIER LIBRARY

SECRETORY AMELOBLASTS AND CALCIUM DISTRIBUTION DURING NORMAL AND EXPERIMENTALLY ALTERED MINERALIZATION

S.H. Ashrafi, D.R. Eisenmann*, A.E. Zaki

Department of Histology, College of Dentistry
801 South Paulina Street
Chicago, Illinois 60612

Abstract

The distribution of calcium in relation to secretory ameloblasts of the rat incisor was studied. An experimental model system in which enamel mineralization was temporarily inhibited by injecting sodium fluoride and cobalt chloride was used. Potassium pyroantimonate (PPA) cytochemistry, electron energy loss spectroscopy (EELS), and energy dispersive X-ray spectrometry (EDS) were used to clarify the role of the ameloblast in controlling calcium distribution during normal and experimentally altered enamel mineralization.

Secretory ameloblasts chemically-preserved in glutaraldehyde either with or without PPA were analyzed for calcium; those preserved with PPA showed higher concentrations of calcium than did those preserved with glutaraldehyde only.

Freeze-dried control and experimental tissues showed an increasing gradient of calcium from stratum intermedium cells to the distal ends of the ameloblasts. Calcium levels were reduced near the distal ends of the cells following fluoride and cobalt injections, while magnesium levels were increased markedly in the same region.

This multi-method approach showed correlated calcium localization in specific regions of this cell in relation to changes in function. The study thus provides additional evidence for active involvement of the ameloblasts in enamel mineralization.

Introduction

While the secretory ameloblast is known to be responsible for secretion of the organic matrix of enamel, it is also believed to be involved in mineralization of enamel, the hardest of all biological tissues. [45]CA autoradiography has been used to demonstrate that the route taken by calcium during mineralization is via the enamel organ (Reith & Cotty, 1962). Experimental evidence from in vitro studies of [45]Ca uptake also indicates that calcium transport to the enamel front is cell-regulated (Bawden and Wennberg, 1977).

Calcium distribution and transport across the ameloblast layer during enamel formation has been the subject of intense research (Wennberg and Bawden, 1978; Karim and Warshawsky, 1979; Bawden and Wennberg, 1979; Boyde and Reith, 1977 and 1978; Reith and Boyde, 1978; Eisenmann et al., 1979; Engel, 1981; Eisenmann et al., 1982; Crenshaw and Takano, 1982; Engel and Hilding, 1984; Zaki et al., 1986; El-Zainy et al., 1987).

Calcium plays a pivotal role in almost every cell type. It has been ascribed the role of a second messenger in controlling cell activities, notably secretion, contraction, conduction, and cell adhesion (Godfreind-DeBecker, 1980; Akerman, 1982).

The localization of diffusible calcium ions in cells and organelles is complicated by technical problems. Freeze-sectioning methods, particularly the recently modified ones, allow for reasonably precise localization in soft tissues, as it is possible to preserve the basic structural form of the cells under study; e.g., nerve (McGraw et al., 1980) and muscle (Somlyo, 1985). However, the application of these methods is very difficult in a highly mineralized tissue such as enamel and its associated forming cells. Even when these methods are applied during the early stage of enamel formation, before it becomes highly mineralized, the cellular morphology is compromised to such an extent that it is difficult to evaluate the result.

Accordingly, we have adopted a multi-method approach which provides complementary results to compensate for the shortcomings of any

individual method. In this review, we will discuss the methods we and others have employed to localize calcium in the ameloblasts during the secretory stage of enamel formation. Our findings as well as related reports and the evaluation of the applied methods will also be presented.

The multi-method approach for identification of cell-related calcium utilized three analytical systems: (1) Potassium Pyroantimonate Cytochemistry (PPA). This method has been used widely for localization and ultrastructural visualization of calcium and other cations (Komnick, 1962; Spicer et al., 1968; DePorter, 1977; Eisenmann et al., 1979; Appleton and Morris, 1979; Wick and Hepler, 1982; Lyaruu et al., 1985; Von Zgliniki and Punkt, 1986; Kogaya and Furuhashi, 1986). (2) Electron Energy Loss Spectroscopy (EELS). This analytical system measures the characteristic energy loss edges for ions such as calcium, and produces elemental imaging showing the distribution of one or more elements in cellular and subcellular structures (Shuman et al., 1982; Jeanguillaume et al., 1984; Arsenault and Ottensmeyer, 1983; Colliex, 1986; and Zaki et al., 1986. (3) Energy Dispersive X-ray Spectrometry (EDS). This method allows identification and quantification of different elements simultaneously in a particular specimen (Hall, 1971). This technique is suitable for analysis of all elements with atomic number greater than five, and has been used to localize calcium in ameloblasts by Boyde and Reith (1977, 1978), Reith and Boyde (1978), Eisenmann et al. (1979, 1982), Engel (1981), Kogaya and Furuhashi (1986), and in cartilage by Appleton et al. (1985).

Experimental Model System

A model system has been developed in which enamel mineralization in the rat incisor is temporarily inhibited by injection of substances such as sodium fluoride and cobalt chloride. This system provides opportunities to assess the calcium concentration of enamel organ tissue during a temporary interruption of enamel mineralization. This disturbance in mineralization was documented microradiographically and ultrastructurally (Neiman & Eisenmann, 1975; Eisenmann et al., 1982). Stippled material accumulated between Tomes' process and the enamel surface. Stippled material has been generally proposed to be enamel matrix (either recently secreted by cells or withdrawn from the enamel); however, a few investigators consider this material a fixation artefact. We have demonstrated that the stippled material in our model system occurs in response to the injected ions and not as a result of post-mortem changes related to quality of fixation (Chen and Eisenmann, 1984). Rats receive a single subcutaneous injection of either 5mg/100 g body weight of sodium fluoride or 12 mg/100 g body weight of cobalt chloride and are killed 1h later for tissue analysis. Tissues are preserved either by perfusion fixation with 2%

glutaraldehyde in 0.05 M PPA, or anhydrously by immediate freezing for 15 seconds in isopentane (-150°C) chilled with liquid nitrogen. The frozen specimens are then transferred into liquid nitrogen and freeze-dried at -35°C in a cryostat vacuum for two days.

In specimens chemically fixed for ultra-structural observation, the secretory ameloblasts (Fig. 1) appear in their well-documented morphology as tall, columnar cells with distal (apical) Tomes' processes in contact with the developing enamel matrix (Warshawsky, 1968, 1986). The proximal (basal) ends of the ameloblasts are in close apposition to the adjacent stratum intermedium cells. The infranuclear region is packed with mitochondria, and the supranuclear region
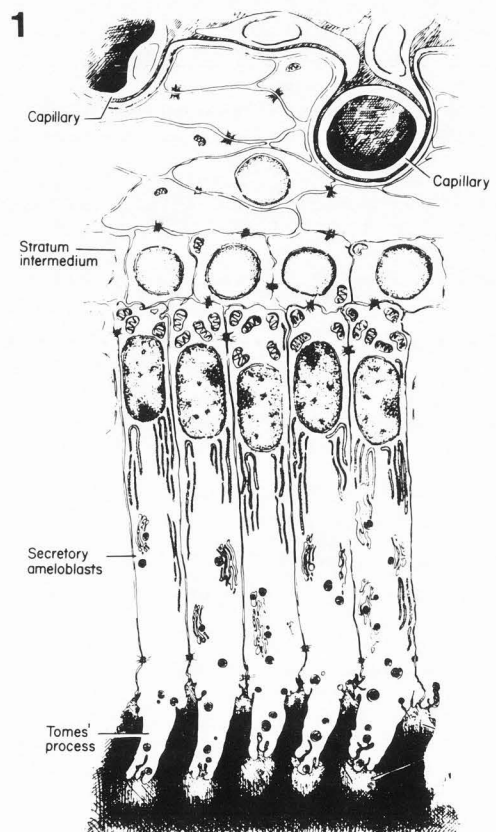

Fig. 1. Diagram of the enamel organ showing tall columnar secretory ameloblasts. Proximal regions of the cells are apposed to the stratum intermedium. The cell comprises an infranuclear region which contains mainly mitochondria. The supranuclear cytoplasm in the central region contains rough endoplasmic reticulum, Golgi and secretory granules, while the distal end consists of Tomes' process with secretory granules. The two secretory regions of Tomes' process are adjacent to regions of experimentally-induced unmineralized enamel labelled "stippled material."

contains a prominent Golgi complex surrounded by rough endoplasmic reticulum,ː coated vesicles, and secretory vesicles which migrate into the Tomes' process. It has been established that the secretory granules release enamel matrix precursors from the Tomes' process secretory regions onto the enamel surface (Matthiessen and Von Bulow, 1969; Weinstock and Leblond, 1971; Slavkin et al., 1976; Karim and Warshawsky, 1979).

Potassium Pyroantimonate Cytochemistry (PPA)

Several investigators have demonstrated localization of calcium in relation to cytologic structures of the secretory ameloblast using PPA cytochemistry (Kuroda, 1977; DePorter, 1977; Appleton and Morris, 1979; Eisenmann et al., 1979; Lyaruu et al., 1985; Reith & Boyde, 1985; Chen et al., 1986). Calcium has been found associated with mitochondria, cell membranes, nuclei, endoplasmic reticulum, secretory granules and other cellular components. We utilized a morphometric approach to determine distribution of calcium pyroantimonate (CaPA) deposits in relation to a number of key cellular components in control and experimentally altered ameloblasts (Chen et al., 1986).

Ultrathin sections were cut from the secretory zone of amelogenesis of the rat incisor for ultrastructural examination. To assess cytological changes and distribution patterns of CaPA deposits following injection of either fluoride or cobalt, the following morphometric parameters were compared: concentration of secretory granules within a fixed area in both the Golgi and Tomes' process regions and percentage of those secretory granules with associated CaPA deposits, concentration of individual CaPA deposits located on mitochondria in the proximal region, numbers of CaPA deposits per linear unit of cell membrane in proximal and central (midcellular) regions, and total area of stippled material in the proximal and distal secretory regions of Tomes' process.

The distribution of CaPA deposits in five control animals served as a baseline for comparison with cells from the injected experimental animals (5 fluoride and 5 cobalt) in which the normal enamel mineralization was temporarily disturbed. In some cases, several adjacent thin sections from PPA-treated animals were decalcified in 5mM EGTA [ethylene glycol bis-(B-aminoethyl ether),N,N,N',N' tetracetic acid], at 60°C prior to ultrastructural examination to confirm the presence of calcium in PPA deposits (Eisenmann et al., 1979).

Morphometric evaluation of the parameters under study allowed comparison of various cytologic structures and associated calcium between control and experimental animals (Table 1). The heaviest CaPA deposits in secretory ameloblasts from control animals occurred in relation to the cell membranes (Fig. 2).

Calcium in Secretory Ameloblasts

Table 1. Mean values of Ca-PA counts in various areas of secretory ameloblasts treated with fluoride and cobalt

Morphometric parameters	Control	Fluoride	Cobalt
Ca-PA in mito-chondria/μm^2	6.37 ± 1.11	4.46 ± 0.74	8.70 ± 0.87
Ca-PA on plasma membrane/μm			
proximal	4.37 ± 0.28	4.40 ± 0.38	4.45 ± 0.44
central	4.79 ± 0.30	5.05 ± 0.55	$3.63 \pm 0.48*$
Change of membrane Ca-PA from proximal to central regions[a]	$+9.6\%$	$+14.7\%$	$-18.3\%*$
Number of SG			
in Golgi/40 μm^2	11.76 ± 0.92	10.72 ± 0.68	$8.04 \pm 0.48**$
in Tomes'/process	11.99 ± 1.58	$28.92 \pm 2.13**$	$15.65 \pm 1.01*$
Number of SGs with Ca-PA			
in Golgi/40 μm^2	3.06 ± 0.40	2.61 ± 0.21	$1.52 \pm 0.17**$
in Tomes'/process	3.83 ± 0.42	4.37 ± 0.51	$1.70 \pm 0.22**$
Percent of SG with Ca-PA			
in Golgi area	25.76 ± 2.17	25.20 ± 1.76	$18.55 \pm 1.18**$
in Tomes' process	19.44 ± 1.58	15.57 ± 1.56	$10.42 \pm 1.03**$
Change of SG with Ca-PA from Golgi region to Tomes' process[a]	$-6.3\%**$	$-9.6\%**$	$-8.1\%**$
Amount of unmin-eralized matrix at secretory regions	0.07 ± 0.02	$0.77 \pm 0.10**$	$0.37 \pm 0.09**$

SG = Secretory granules.
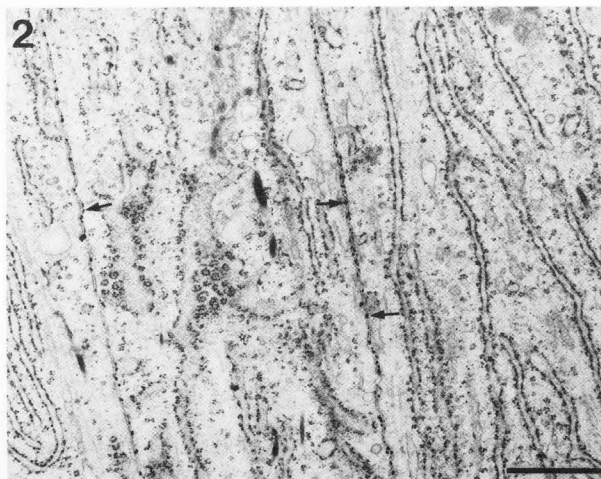* $p < 0.05$; ** $p < 0.01$.
[a] Compared within individual cell.

Fig. 2. Central region of the secretory ameloblast showing several Ca-PA deposits along the cell membranes (arrows). Scale Bar = 1μm.

Many of the deposits appeared to be aligned along the cytoplasmic side of the membrane, and this localization was observed in both normal specimens (Fig. 3a) and in experimentally altered ones (Fig. 3b). Some were also along the outer surface. Concentrations of CaPA in the mitochondria showed no differences between controls and experimentals (Fig. 4). The most distinct difference in fluoride-injected animals consisted of a significant increase in the number of secretory granules in Tomes' process and the accumulation of substantial amounts of stippled material at the secretory regions (Fig. 5) as compared with normal (Fig. 6).

In the cobalt-injected specimens marked disturbances in calcium concentration were observed. Fewer CaPA deposits were present along the cell membranes and in association with secretory granules in both the Golgi and Tomes' process regions (Fig. 7). Substantial amounts of stippled material were observed at both proximal and distal secretory regions of Tomes' process (Fig. 8).

Energy Dispersive X-ray Spectrometry (EDS)

Previous investigators (Boyde and Reith, 1977; Reith and Boyde, 1978) applied EDS to rat molar and incisor teeth and found very low levels of calcium (based on calcium peak height) in association with the ameloblasts. Engel (1981), on the other hand, observed substantially higher concentrations in the developing mouse molars. We used this micro-analytical method to investigate calcium distribution in sections of the enamel organ cells in chemically preserved tissue (PPA cytochemistry method) as well as in freeze-dried blocks of enamel organ tissue.

Calcium analyses were performed in a Cambridge stereoscan S4-10 microscope attached to a computerized energy dispersive X-ray EDAX analyzer system. Spectra were recorded in the range of 0.0-8000 eV, with 20 eV per channel. The operating conditions of the analyzer were 100 seconds for recording spectra at 20 kV and 160 µA beam current. The tilt angle for thin sections was 10° and take off angle was 6.7°. The tilt angle for bulk specimens was 45°, and take off angle was 30°. The beam size was around 100 nm. The calcium peak was recorded at 3,700 eV. The element counts per 100 seconds and peak to background ratio of calcium counts per 100 seconds were determined by using a computer-run EM program supplied by EDAX International. The computer program subtracted background and corrected for overlapping of elemental peaks.

Small strips of enamel organ were dissected from mid-sagittal slices of rat incisors perfused with 2% glutaraldehyde with or without 0.5M PPA (Eisenmann et al., 1982), and immediately frozen in liquid nitrogen, chilled in isopentane at -150°C and freeze-dried at -35°C in a cryostat under vacuum. Osmium tetroxide was not used for post-fixation
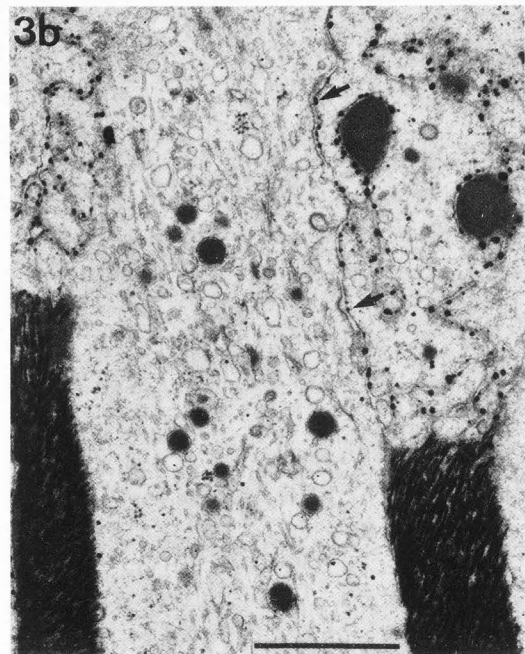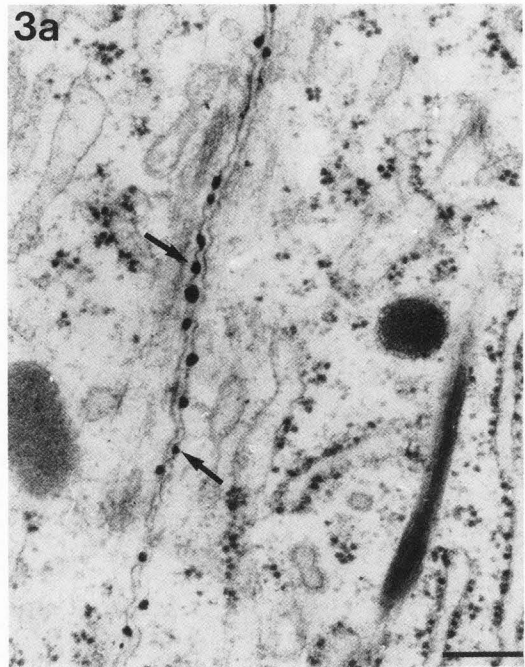

Fig. 3. Higher magnification of the (a) central zone (normal) and (b) distal region (experimental-cobalt) of the secretory ameloblasts showing Ca-PA deposits (arrows) along the cytoplasmic side of the cell membrane. 3a: Scale Bar = 0.2µm. 3b: Scale Bar = 1µm.
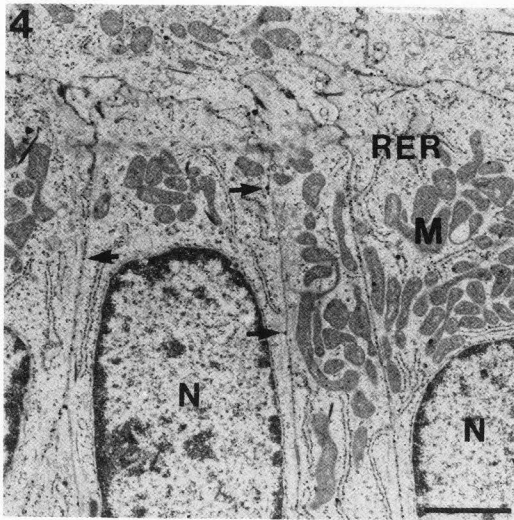
Fig. 4. Proximal region of normal secretory ameloblasts showing CaPA deposits along cell membranes (arrows) in mitochondria (M), in rough endoplasmic reticulum (RER) and in nucleus (N). Scale Bar = 2μm.
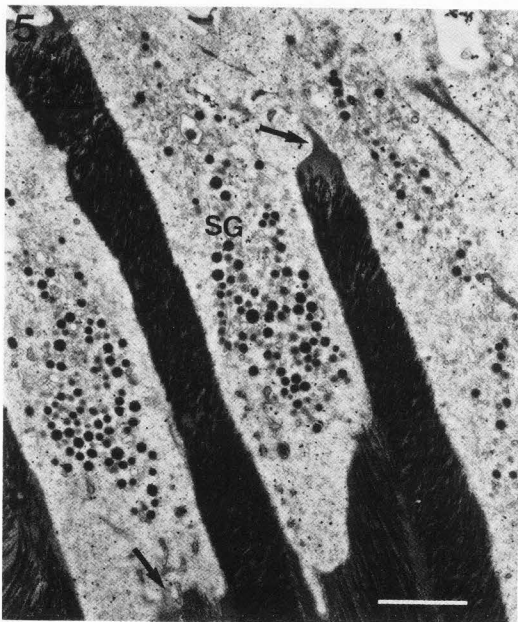

Fig. 5. Tomes' process of ameloblast from fluoride injected animal. Increased numbers of secretory granules (SG) are present. Stippled material is also seen at both proximal and distal secretory regions (arrows). Scale Bar = 2μm.
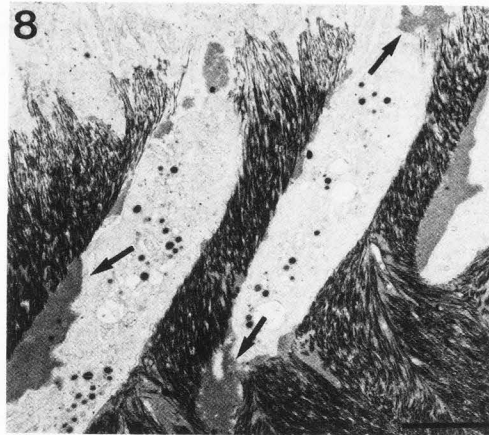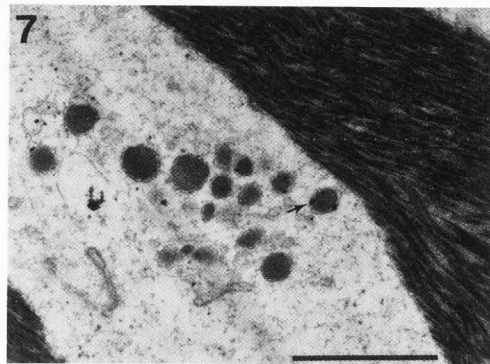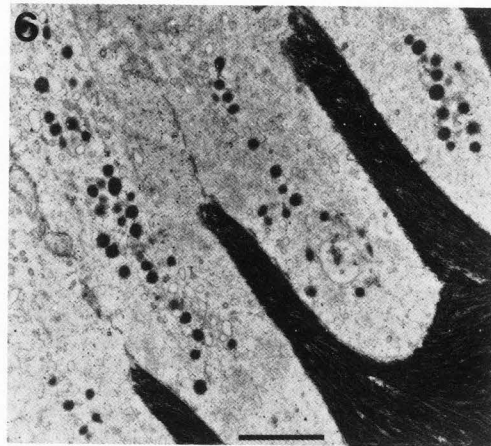
Fig. 6. Tomes' process of ameloblasts from normal rat incisor. Typical numbers of secretory granules are present. Very little stippled material is observed on the surface of forming enamel. Scale Bar = 2μm.

Fig 7. Tomes' process region of ameloblasts from cobalt-treated animal. CaPA deposits are present in association with secretory granules (arrow). Scale Bar = 1μm.

Fig. 8. Tomes' process region from cobalt-injected animal. Substantial amounts of stippled material are observed in various locations around Tomes' process (arrows). Scale Bar = 2μm.

of these tissues. Although the freezing produced ice crystals and left artefactual holes in the range of 0.1-0.5 µm in diameter, this should not have affected the results, as the microanalytical area used was 8x8 µm with a spatial resolution of around 10-15µm. The specimens were mounted on a carbon stud and coated with evaporated carbon to a thickness of 40 nm before X-ray microanalysis.

A minimum of ten readings was recorded from each sample. Under the operating conditions described, the analytical volume covered approximately two to three cells in width as well as depth.

To avoid calcium ion dislocation due to chemical treatment and fixation, some enamel organ tissue from normal, fluoride, and cobalt-injected rats (3 animals in each group) was preserved anhydrously (Eisenmann et al., 1984). Upper incisors and their adherent alveolar bone were dissected quickly from surrounding tissues. The incisor was partially dislocated from its socket by manual pressure which caused a separation to occur between the distal ends of the ameloblasts and the forming enamel surface. Separation of the cells from the mineralized enamel permits elemental analysis of their most distal portions without picking up contaminating Ca signals from the enamel. The incisor was then immediately frozen and freeze-dried under vacuum for two days. After drying, the enamel organ was separated from adjacent tissues using micro-dissection techniques. Only enamel organ tissue in the secretory zone (as determined by measurements) was used. The freeze-dried enamel organs were fractured in a plane parallel to the long axis of the tooth, exposing the lateral surface of the tall columnar ameloblasts and the adjacent rounded stratum intermedium cells, as described previously (Skobe, 1976; and Boyde and Reith, 1976). This lateral surface, as well as the distal ends of the separated ameloblasts, were used for microanalysis (Fig. 9).

EDS analysis of PPA deposits in the sections revealed calcium and antimonate peaks in the proximal mitochondrial compartment and the supranuclear region. Spot analysis of PPA deposits on the cell membrane indicated the presence of both calcium and antimonate. Analysis of sections decalcified in EGTA demonstrated neither antimony nor calcium peaks.

EDS analysis of the distal surface of freeze-dried enamel organ tissue fixed initially with glutaraldehyde showed a lower concentration of calcium than that fixed initially with glutaraldehyde containing PPA (Figs. 10, 11). Chemically-fixed enamel organs always contained lower levels of calcium than those preserved by freeze-drying only (Eisenmann et al., 1982).

Recently, quantitative autoradiographic data showed that PPA-processed developing teeth retained significantly more [45]Ca than similar tissues processed without PPA (El-Zainy et al., 1987). It appears that PPA complexes retain loosely bound calcium which would otherwise be lost during tissue processing.
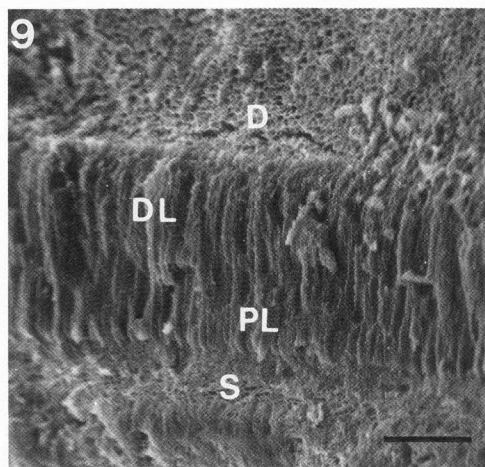

Fig. 9. Scanning electron micrograph of freeze-dried enamel organ showing the regions used for X-ray microanalysis. Three of the analytical regions, stratum intermedium (S), proximal lateral surface (PL), and distal lateral surface (DL) are indicated on the lateral fractured surface. The fourth region, distal end (D) of the ameloblasts consists of the surface of the enamel organ which was previously in contact with the forming enamel. Scale Bar = 30µm.
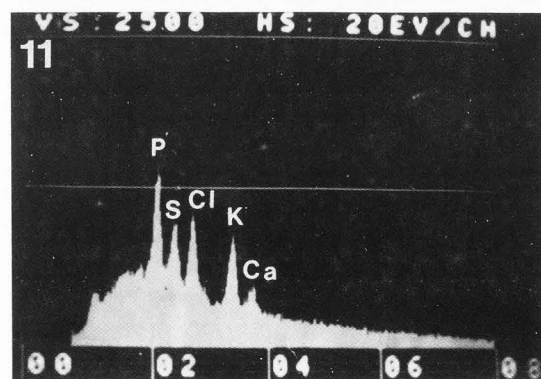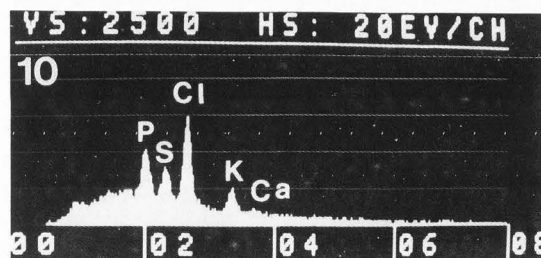

Fig. 10. EDS analysis of enamel organ fixed with glutaraldehyde alone. Some calcium was lost during processing.
Fig. 11. EDS analysis of enamel organ fixed with glutaraldehyde containing PPA. Greater portion of calcium was retained by PPA.

Secretory ameloblasts and adjacent stratum intermedium cells could be readily distinguished on the lateral fractured surface of the freeze-dried enamel organs. EDS of those tissues preserved entirely by this anhydrous method revealed a gradation of calcium concentration in the four regions analyzed (Fig. 12). All specimens, both control and experimental (cobalt or fluoride-injected), showed a progressive increase in calcium levels from the stratum intermedium to the distal ends of the ameloblasts. A marked reduction in calcium levels occurred in response to both fluoride and cobalt with the greatest reduction following cobalt. This reduction was greatest near the distal ends of the ameloblasts and was statistically significant in this area. The vertical scale, VS:2500, was kept constant to enable comparison of the peaks in Figs. 13, 14 and 15. Thus, lower calcium peaks in fluoride specimens (Fig. 13) and cobalt specimens (Fig. 14) as compared with controls (Fig. 15) indicate reduced calcium concentrations in enamel organ tissue where mineralization had been temporarily inhibited.

EDS of magnesium was also carried out on the fractured lateral and detached distal surfaces of the freeze-dried enamel organ tissue. The levels of calcium and magnesium were inversely related in control and experimental specimens (Fig. 16). Thus, magnesium was found to increase relative to calcium in enamel organ tissue under the influence of either fluoride or cobalt.
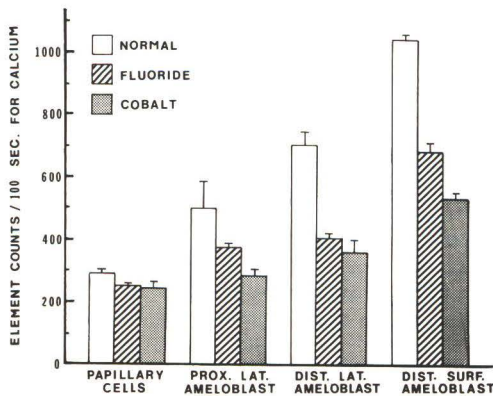
Fig. 12. Histogram of element counts/100 sec. for calcium in four analytical regions. Calcium concentration is reduced by fluoride and cobalt injection and most noticeably near the distal ends of the secretory ameloblasts.
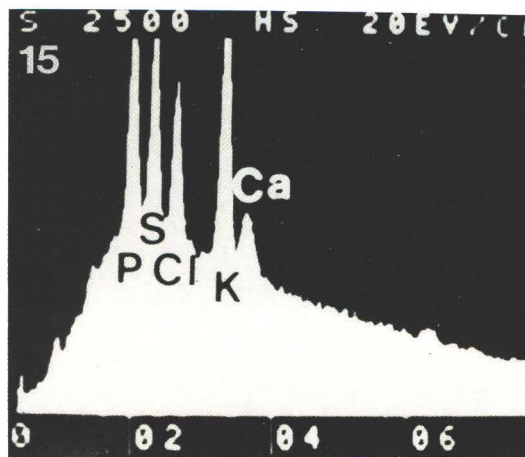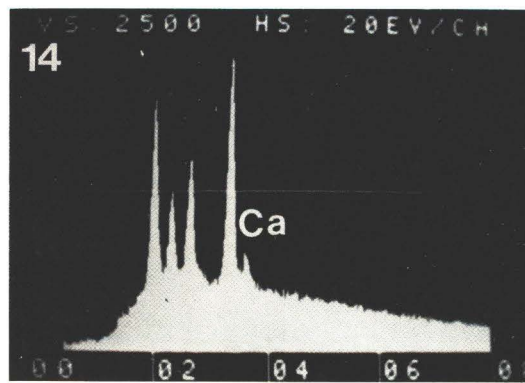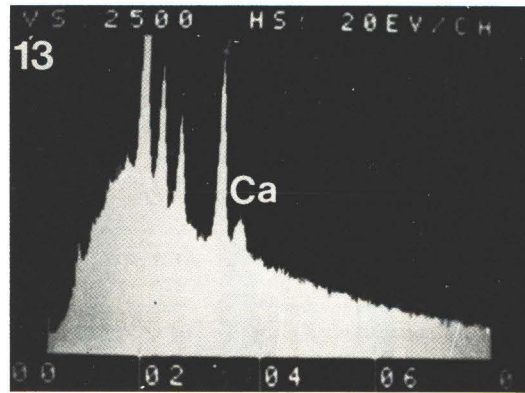
Fig. 13. EDS analysis of the distal surface of the freeze-dried enamel organ from an animal treated with fluoride (Calcium peak Ca).

Fig. 14. EDS analysis of the distal surface of a freeze-dried enamel organ from a cobalt injected rat. The concentration of calcium was lower than in fluoride treated animals.

Fig. 15. EDS analysis of the distal surface of freeze-dried enamel organ from control animals. Calcium peak reads higher than in fluoride and cobalt injected animals.

Fig. 16. Histogram of calcium and magnesium counts from the distal surface of the freeze-dried enamel organs of the normal, fluoride and cobalt treated rat incisors.
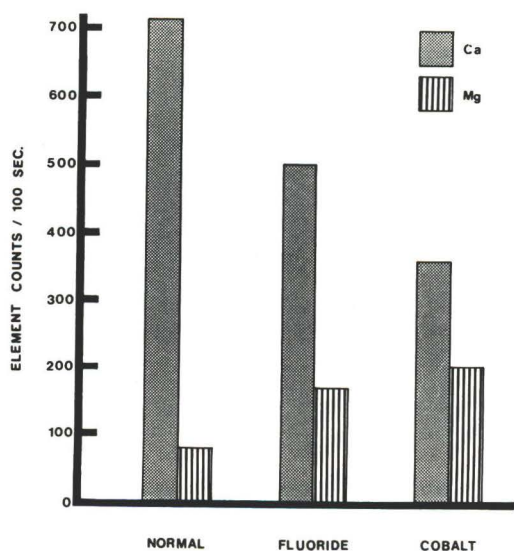

Fig. 17. Electron energy loss spectrum of CaPA deposits in the secretory ameloblast, showing separate edges from calcium (Ca L23) and antimony (Sb M45).

Electron Energy Loss Spectroscopy (EELS and Elemental Imaging

EEls has an intrinsically higher resolution as well as a higher sensitivity for low atomic number elements which cannot be normally detected with EDS (Leapman, 1982). EELS measures the characteristic energy loss "edges" in a beam of fast electrons when inner shell levels of atoms in the sample are excited or ionized. In addition, EELS imaging produces
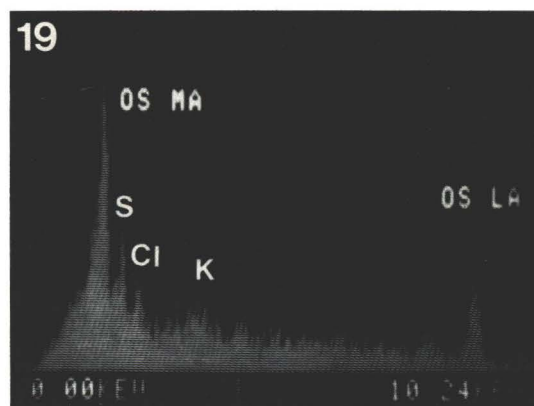

Fig. 19. EDS analysis of the stippled material found near Tomes' process of ameloblast/enamel from a fluoride-injected rat. Calcium was not localized in the stippled material.

quantitative elemental distributions with a resolution capable of distinguishing different intracellular and extracellular sites. Analysis of secretory granules containing PPA revealed the presence of the Ca $L_{2,3}$ edge at 348 eV and the antimony $M_{4,5}$ edge at 530 eV (Fig. 17). Quantitative analysis of the EELS spectra indicated that the composition of the PPA deposit was consistent with that of calcium pyroantimonate. This confirmed the validity of the PPA cytochemistry method.

Similar opbservations were made in the spectra from deposits along the ameloblast cell membranes, but calcium was not detected in the mitochondria present in the proximal end of the secretory ameloblast. The application of STEM-EELS mapping was demonstrated in calcium imaging of a region in Tomes' process from a PPA-treated sample. Elemental imaging did not show the presence of calcium in stippled material from fluoride (Fig. 18) and cobalt-injected specimens. Consistent with the presumed protein composition of this material, nitrogen was present. EDS analysis of the stippled material also did not show calcium. The stippled material did produce the peaks for sulfur and chlorine (Fig. 19).

Correlation of Results from Analytical Methods

Limitations of PPA Cytochemistry

Several limitations have been noted with regard to application of cytochemical methods for preserving and localizing calcium in tissues (Reith and Boyde, 1978; Van Iren et al., 1979; Caswell, 1979; Landis and Glimcher, 1982; Von Zglinicki and Punkt, 1986). For example, considerable translocation of calcium ions can occur during chemical fixation of the tissue.
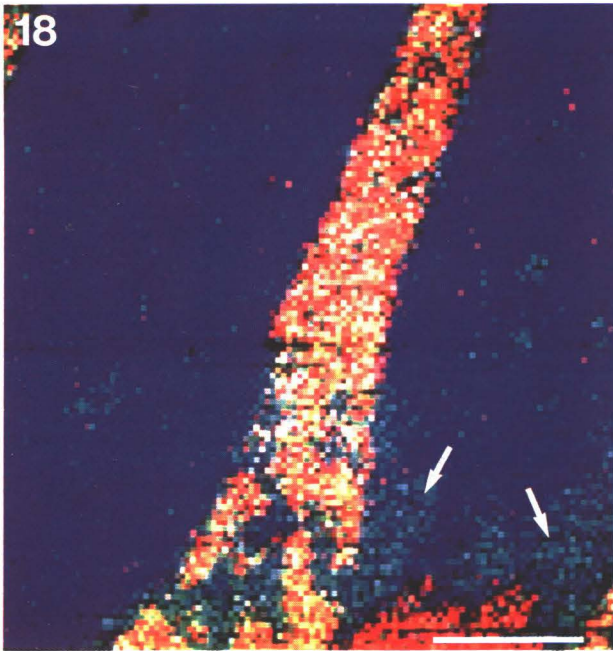
Fig. 18. Scanning transmission electron microscope elemental mapping by electron energy loss spectroscopy of Tomes' processes of secretory ameloblasts from a fluoride injected rat. The elemental distribution of nitrogen is shown in green; calcium in red; carbon in blue. Note the areas of unmineralized enamel matrix (stippled material) at the ameloblast/enamel interface (arrows). Scale Bar = 1μm.

However, the careful choice of reaction conditions and the inclusion of adequate controls enhance the usefulness of the PPA technique as an indicator of calcium distribution (Wick and Hepler, 1982; Reith and Boyde, 1985; Lyaruu et al., 1985; Kogaya and Furuhashi, 1986). It should be stressed that in our work, the pyroantimonate technique was primarily used for comparative purposes between experimental and control conditions. Also the results were interpreted in conjunction with the data from other methods such as analysis of freeze-dried specimens and electron energy loss spectroscopy (Eisenmann et al., 1982; Kogaya and Furuhashi, 1986; Makita and Hakoi, 1986; Zaki et al., 1986). Further, adequate controls such as elemental analysis of PPA deposits and the examination of demineralized sections were employed.

Secretory Granule-Associated Calcium

Cytochemically localized calcium in association with the organelles involved in synthetic activities was confirmed by our studies as well as by those of others (DePorter, 1977; Reith and Boyde, 1978; Lyaruu et al., 1985; Koyaga and Furuhashi, 1986; Chen et al., 1986) which correlates with earlier observation of

the same distribution using ^{45}Ca electron microscopic autoradiography (Nagai and Frank, 1975). Calcium was detected in association with secretory granules by PPA cytochemistry, EDS and EELS analyses. This may indicate processing of calcium along with organic matrix components of enamel which could then be released at the mineralizing front by exocytosis. Although the volume of calcium transported by this method appears to be very small, it may play a role in crystal initiation on the forming surface of enamel.

Cell Membrane-Associated Calcium

The predominant demonstration of cell associated calcium in secretory ameloblasts has been found cytochemically (Kuroda, 1977; Eisenmann et al.,1979; Reith and Boyde, 1985; Lyaruu et al., 1985; Koyaga and Furuhashi, 1986) and autoradiographically (Nagai and Frank, 1975) to be in association with the cell membranes. Reith (1983) has proposed a translational movement of calcium within the ameloblast cell membrane with phosphatidylserine as the calcium carrier. Reith and Boyde (1985) also proposed an alternative model in which calcium ions roll along the inner surface of the lipid membrane in their transit from the blood supply to the enamel mineralizing front. This hypothesis finds support in observations made in application of PPA cytochemistry to the secretory ameloblast. Enamel mineralization experimentally inhibited by cobalt is followed by a reduction in membrane-associated calcium (Chen et al., 1986). The gradient of increasing calcium concentration in the EDS studies of freeze-dried enamel organ tissue is most likely representative of membrane-associated calcium, since this localization is cytochemically predominant in these cells; and indeed, intracellular calcium levels are known to be quite low (10^{-7}M, Akerman, 1982). When the animals are subjected to either fluoride or cobalt, there is a marked reduction in this calcium gradient, especially near the distal ends of the ameloblasts (Eisenmann et al., 1984). This may be evidence of an important dynamic gradient at play in the translocation within or in association with the membrane of these cells.

Cobalt Model System

The cobalt-induced alterations in ameloblasts and their product show promise as a model system which merits further study. Previous studies of the inhibitory effects on mineralization of fluoride and cobalt indicate differences in responses to these ions (Neiman and Eisenmann, 1975). During the active fluoride response, there is an inhibition of formation of new crystals, whereas preinjection enamel continues to accumulate mineral. The response to cobalt is more profound: new crystal formation and increased mineral density of deeper layers are inhibited. This corresponds with our observation by cytochemistry and elemental analysis that cobalt caused a greater decrease in enamel organ calcium than did fluoride. It appears

that crystal growth in deeper layers continues in the presence of moderately reduced levels of calcium in enamel organ tissue (fluoride response), but that it is inhibited when there is a greater reduction in calcium (cobalt response). Although the exact mechanisms of cobalt's action are unknown, there are several possibilities which may be considered. Cobalt is known to inhibit calcium entry into cells (Baker, 1976), and to exert a number of other effects, including tissue hypoxia (Smith et al., 1974) and disturbances in mitochondrial respiration (DeMoraes and Mariano, 1967). Bawden and Crenshaw (1984) observed a 50% reduction in uptake of calcium by enamel in organ culture of tooth germs exposed to cobalt. Conversely, our recent cytochemical studies of the effect of cobalt on $Ca^{2+}-Mg^{2+}$ ATPase in relation to the ameloblast has demonstrated an increased level of enzyme activity at the same time that enamel mineralization is being inhibited (Salama et al., 1987).

It has been reported that although cobalt activates $Ca^{2+}-Mg^{2+}$ ATPase activity, it interferes with the formation of the phosphorylated intermediate of $Ca^{2+}-Mg^{2+}$ ATPase called phosphoenzyme intermediate, which is a necessary step in the transport reaction for calcium (Pecker and Lotersztajn, 1985). Therefore, the blockade of phosphoenzyme formation due to the presence of cobalt ions could interfere with calcium transport in relation to the secretory ameloblast cell membrane as required for mineralization of enamel.

Although it is not clear which mechanism(s) are being targeted by cobalt, its remarkable effectiveness in altering cell-associated calcium justifies its continued use for investigating cellular control of enamel mineralization.

Benefits of Combined EELS and EDS Analysis

Most of the secretory granules fixed without PPA did not show a calcium edge in the EELS spectra. However, EDS analysis of such granules revealed the presence of calcium. To exclude the effect of scattered electrons giving rise to remotely excited X-rays from calcium in the adjacent enamel, areas of Tomes' process between secretory granules were also analyzed. The resulting spectra exhibited only a weak calcium peak which may partly be explained by remote excitation. It is unlikely that the stronger calcium peak resulting from the secretory granule analysis is solely due to remote excitation.

The advantage of EELS is the strong signal which results from the inherently large collection efficiency for inelastic scattering. The high counting ratio, typically 10^6 counts per second for a pure element in the 200-500eV region, makes feasible EELS elemental mapping. Counting rates in EDS are generally orders of magnitude lower, making it difficult to obtain elemental images at all. However, EDS has the advantage of high peak/background

ratios. Conversely, EELS generally superimposes the characteristic core edges on a large background arising from excitation of lower energy core levels in the sample. This limits the minimum mass fraction of an element which can be reliably detected in a biological matrix. Such considerations can explain why it was not possible to detect calcium in secretory granules of ameloblasts prepared without PPA using EELS in our experimental system, while EDS did reveal calcium in a point analysis.

Thus, the combined use of EELS and EDS in our multi-method analysis provided several advantages. These were a wide range of elemental analyses in a complex mineralizing tissue, as well as elemental imaging capability and further validation for the use of EDS in CaPA analysis, as EELS clearly demonstrated distinct edges for Ca and Sb.

Conclusion

Multiple methods and experimental approaches are necessary for investigating a difficult question such as the involvement of the ameloblast in mineralization of enamel. Analysis of calcium distribution in chemically preserved tissues is fraught with the uncertainties created by dislocation of calcium ions from their natural positions. Freeze-dried preparations permit more accurate localization of diffusible substances, but much of the morphological detail of the tissues is lost. Systems for elemental and cytochemical analyses have their respective limitations, but can be very useful when applied on a comparative basis. Multi-method elemental analysis of chemically-fixed and freeze-dried specimens showed an increasing gradient of calcium from the stratum intermedium cells to the distal ends of the secretory ameloblast facing the mineralizing enamel front. Calcium concentration at these sites was reduced following fluoride and cobalt injections, while magnesium levels increased markedly in the same region. Much remains to be learned about control of calcium transport and uptake by mineralizing enamel. Correlation of data derived from a broad range of experimental systems and approaches offers the best potential for reaching a better understanding of the mechanisms involved.

Acknowledgements

References

Akerman KEO (1982) Ca^{2+} transport and cell activation. Med. Biol. 60: 168-182.

Appleton J, Morris DC (1979) The use of potassium pyroantimonate-osmium method as a means of identifying and localizing calcium at the ultrastructural level in the cells of calcifying systems. J. Histochem. Cytochem. 27: 676-680.

Appleton J, Lyon R, Swindin KJ, Chester J (1985) Ultrastructure and energy dispersive x-ray microanalysis of cartilage after rapid freezing, low temperature freeze-drying, and embedding in Spurr's resin. J. Histochem. Cytochem. 33: 1073-1079.

Arsenault AL, Ottensmeyer FP (1983) Quantitative spatial distributions of calcium, phosphorus, and sulfur in calcifying epiphysis by high resolution electron spectroscopy imaging. Proc. Nat'l. Acad. Sci. U.S.A. 80: 1322-1326.

Baker PE (1976) The regulation of intracellular calcium pump. Symp. Soc. Exp. Biol. 30: 67-88.

Bawden JW, Crenshaw MA (1984) Effect of inhibition of net calcium uptake on net fluoride uptake in developing rat molars. J. Dent. Res. 63: 642-645.

Bawden JW, Wennberg A (1979) Ameloblasts-Ion transport function. J. Dent. Res. 58: 708-713.

Bawden JW, Wennberg A (1977) In vitro study of cellular influence on Ca uptake in developing rat enamel. J. Dent. Res. 56: 313-319.

Boyde A, Reith EJ (1978) Electron probe analysis of maturation ameloblasts of the rat incisor and calf molar. Histochemistry. 5: 41-48.

Boyde A, Reith EJ (1977) Quantitative electron probe analysis of secretory ameloblasts and odontoblasts in the rat incisor. Histochemistry 50: 347-354.

Boyde A, Reith EJ (1976) Scanning electron microscopy of the lateral cell surfaces of rat incisor ameloblasts. J. Anat. 3: 603-610.

Caswell AH (1979) Methods of measuring intracellular calcium. Int. Rev. Cytol. 56: 146-181.

Chen S, Eisenmann DR (1984) Ultrastructural study of the effects of fixation and fluoride injection on stippled material during amelogenesis in the rat. Archs. Oral Biol. 29: 681-686.

Chen S, Eisenmann DR, Zaki AE, Ashrafi SH (1986) Cytochemical calcium distribution in secretory ameloblasts of the rat in relation to enamel mineralization. Acta. Anat. 126: 34-40.

Colliex C (1986) Electron energy-loss spectroscopy analysis and imaging of biological specimens. Ann. N.Y. Acad. Sci. 483: 311-325.

Crenshaw MA, Takano Y (1982) Mechanisms by which the enamel organ controls calcium entry into the developing enamel. J. Dent. Res. 61: 1574-1579.

DeMoraes S, Mariano M (1967) Biochemical aspects of cobalt intoxication. Med. Pharm. Exp. 16: 441-447.

DePorter DA (1977) The early mineralization of enamel. Fine structural observations on the cellular localization of calcium with the potassium pyroantimonate technique. Calcif. Tiss. Res. 24: 271-274.

Eisenmann DR, Ashrafi S, Zaki AE (1984) Calcium distribution in freeze-dried enamel organ tissue during normal and altered enamel mineralization. Calc. Tissue Int. 36: 596-603.

Eisenmann DR, Ashrafi S, Zaki AE (1982) Multimethod analysis of calcium localization in the secretory ameloblasts. J. Dent. Res. 61: 1555-1561.

Eisenmann DR, Ashrafi S, Neiman A (1979) Calcium transport and the secretory ameloblasts. Anat. Rec. 193: 403-422.

El-Zainy MA, Zaki AE, Eisenmann DR (1987) Comparisons of processing with and without potassium pyroantimonate in quantitative autoradiography of calcium in developing teeth of the frog Rana pipiens. Arch. Oral Biol. 32: 143-149.

Engel MB (1981) Microprobe analysis of calcifying matrices and formative cells in developing mouse molars. Histochemistry 72: 443-452.

Engel MB, Hilding OH (1984) Mineralization of developing teeth. Scanning Electron Microscopy, 1984; IV: 1833-1845.

Godfreind-DeBecker A (1980) Calcium transport: A comparative study in different cells. Int. Rev. Cytol. 67: 141-170.

Hall TA (1971) Microprobe assay of chemical elements, In: Physical Techniques in Biological Research, 2nd ed. Oster, G. ed. Vol. 1, pp. 157-272, Academic Press, N.Y.

Jeanguillaume C, Berry JP, Colliex C, Galle M, Tenee M, Trebbia P (1984) Recent results in EELS elemental mapping of thin biological sections. J. de Phys. Suppl. Coll. 45:C2: 577-580.

Karim A, Warshawsky H (1979) The effect of colcemid on the structure and secretory activity of ameloblasts in the rat incisor as shown by autoradiography after injection of ^{3}H-proline. Anat. Rec. 195: 587-609.

Kogaya Y, Furuhashi K (1986) The difference in calcium distribution pattern between preodontoblasts and preameloblasts in developing rat molar tooth germs. Calcif. Tiss. Int. 39: 78-85.

Komnick H (1962) Elektron microskopische lokalisation von Na^{+} and Cl^{-} in Zellen and Geweben. Protoplasma 55: 414-418.

Kuroda S (1977) Electron microscopic localization of ionic calcium in ameloblasts. J. Dent. Res. 56B: 132.

Landis WJ, Glimcher MJ (1982) Electron optical analytical observations of rat growth plate cartilage prepared by ultra-microcryotomy: the failure to detect mineral phase in matrix vesicles and identification of heterodispersed particles as the initial solid phase of calcium phosphate deposits in the extracellular matrix. J. Ultrastruct. Res. 78: 227-268.

Leapman RD (1982) Application of electron energy loss spectroscopy in biology: Detection of calcium and fluorine. Proc. 40th Ann. Mtg. Electron Micros. Soc. Amer., Claitor's Publishing Division, Baton Rouge, pp. 412-415.

Lyaruu DM, Bronckers AL, Burger EH, Woltgens JHM (1985) Localization of calcium in differentiating early dentinogenesis and amelogenesis in hamster tooth germs. J. Histochem. Cytochem. 33: 595-603.

Makita T, Hakoi K (1986) Advantageous usage of EELS to detect Ca in pyroantimonate staining. Acta Histochem. Cytochem. 19: 289-295.

Matthiessen ME, Von Bulow FA (1969) The ultrastructure of human secretory ameloblasts. Z. Zellforsch. 101: 232-240.

McGraw C, Somlyo AV, Blaustein MP (1980) Localization of calcium in presynaptic nerve terminals: An ultrastructural and electron microprobe analysis. J. Cell Biol. 85: 228-241.

Nagai N, Frank RM (1975) Transfert du Ca par antoradiographie en microscopie electronique au cours de l'amelogenese. Calcif. Tiss. Res. 19: 211-221.

Neiman A, Eisenmann DR (1975) The effect of strontium, cobalt and fluoride on rat incisor enamel formation. Anat. Rec. 183: 303-322.

Pecker F, Lotersztajn S (1985) Fe^{2+} and other divalent metal ions uncouple Ca^{2+} transport from $Ca^{2+}-Mg^{2+}$ ATPase in rat liver plasma membranes. J. Histochem. Cytochem. 260: 713-735.

Reith EJ (1983) A model for transcellular transport of calcium based on membrane fluidity and movement of calcium carriers within the more fluid microdomains of plasma membrane. Calcif. Tissue Int. 35: 129-134.

Reith EJ, Boyde A (1985) The pyroantimonate reaction and transcellular transport of calcium in rat molar enamel organ. Histochemistry 83: 539-543.

Reith EJ, Boyde A (1978) Histochemical and electron probe analysis of secretory ameloblasts on developing rat molar teeth. Histochemistry 55: 17-26.

Reith EJ, Cotty VG (1962) Autoradiographic studies on calcification of enamel. Arch. Oral Biol. 7: 365-372.

Salama AH, Zaki AE, Eisenmann DR (1987) Effect of cobalt on $Ca^{2+}-Mg^{2+}$ ATPase on rat incisor ameloblasts. J. Dent. Res. 66(Sp. Iss.): 142.

Shuman H, Somlyo AV, Somlyo AP, Frey T, Safer D (1982) Energy loss imaging in biology. Proc. 40th EMSA, Claitor's Publishing Division, Baton Rouge, pp. 416-419.

Skobe Z (1976) The secretory stage of amelogenesis in rat mandibular incisor teeth observed by scanning electron microscopy. Calcif. Tiss. Res. 21: 83-103.

Slavkin HC, Mino W, Bringas P (1976) The biosynthesis and secretion of precursor enamel protein by ameloblasts as visualized by autoradiography after tryptophan administration. Anat. Rec. 185: 289-312.

Smith RJ, Ignarro LJ, Heidger PM, Fisher JW (1974) Lysosomal enzyme release in vivo: An evaluation of the mechanics of cobalt polycythemia. J. Pharmacol. Exper. Therap. 191: 564-574.

Somlyo AP (1985) Cell calcium measurement with electron probe and electron energy loss analysis. Cell Calcium 6: 197-212.

Spicer SS, Hardin JH, Greene WB (1968) Nuclear precipitates in pyroantimonate-osmium tetroxide-fixed tissues. J. Cell Biol. 39: 216-221.

Van Iren R, Van Essen-Joolen L, Van der Duyn Schouten P, Boers-Van der Sluiji P (1979) Sodium and calcium localization in cells and tissues by precipitation with antimonate. Histochem. 63: 273-294.

Von Zglinicki T, Punkt K (1986) Localization artifacts in ultracytochemical ion precipitation reactions. Histochem. J. 18: 29-35.

Warshawsky H (1986) Ultrastructural studies on amelogenesis. In: Chemistry and Biology of Mineralized Tissue. (ed.) W.T. Butler, Ebsco Media, Inc., Birmingham, pp. 33-45.

Warshawsky H (1968) The fine structure of secretory ameloblasts in rat incisors. Anat. Rec. 161: 211-230.

Weinstock A, Leblond CP (1971) Elaboration of the matrix glycoprotein of enamel by the secretory ameloblasts of the rat incisor as revealed by autoradiography after galactose-^{3}H-injection. Cell Biol. 51: 26-51.

Wennberg A, Bawden JW (1978) Influence of the pulpal route on uptake of ^{45}Ca in enamel and dentin of developing rat molar. J. Dent. Res. 57: 313-318.

Wick SM, Hepler PK (1982) Selective localization of intracellular Ca with potassium antimonate. J. Histochem. Cytochem. 30: 1190-1204.

Zaki A, Eisenmann DR, Ashrafi S, Leapman R, Fiori C (1986) Energy loss spectroscopic imaging of rat ameloblasts. Prog. in Developmental Biol. Part B ed. Slavkin, H.C., Alan R. Liss, Inc., New York, pp. 215-218.

Discussion with Reviewers

J. Appleton: How is the quality and amount of CaPA precipitate related to the concentration of available ionic calcium? Coarse precipitates may indicate a relatively slow rate of precipitate formation occurring in the presence of low concentration of available calcium ions, while fine precipitates may indicate relatively rapid rates of formation.

Authors: The particle size of the precipitate is related to the rate of precipitate formation. It has been established that smaller precipitate granules are formed as one approaches a higher degree of supersaturation. No marked variations

of particle size were observed in relation to the parameters considered in our studies.

J. Appleton: Although pyroantimonate prevents the loss of some calcium ions, how reliable is a method which involves aqueous fixation in demonstrating the distribution of calcium?
Authors: It is commonly accepted that aqueous fixation undermines the reliability of methods used to demonstrate the distribution of diffusible ions such as calcium. Pyroantimonate demonstrates only that fraction of calcium which is loosely bound and available for precipitation. Free ionic calcium is obviously lost in the aqueous tissue processing. However, it is most likely the loosely bound calcium which is most active in the systems under study. Accordingly, we emphasize that, in spite of the mentioned limitations, the pyroantimonate technique (with adequate controls) is useful to compare calcium localization in cells involved in normal enamel mineralization with those associated with experimentally-altered enamel formation. We have found it to be of value for such comparative purposes and in association with other correlative methods.

J. Appleton: Are you satisfied that the freezing and freeze-drying methods you use inhibit or prevent loss and relocation of calcium ions?
Authors: We are satisfied that our freezing methods minimized the relocation of calcium ions. Rapid dissection and separation of the enamel organ cells from adjacent enamel before freezing are significant contributing factors in preventing loss of calcium ions.

J. Appleton: Have you investigated the distribution of phosphorous or other elements in the ameloblast?
Authors: The distribution of phosphorus (and other elements) is currently under investigation.

G.M. Roomans: For reliable analysis of calcium in your specimens, it is imperative that the spectral overlaps between the Ca K_α line and the K K_α and Sb L_α lines are correctly resolved. In some specimens, you may even have triple overlap. Have you checked how well your deconvolution routine performs; e.g., with model specimens?
Authors: We used stripped elemental analysis (EDIT EM computer program) to correctly resolve the Ca K_α from the K K_α and Sb L_α lines. First we stripped the background from the spectrum. This gave us clear peaks from K K_α and a combined peak for Ca K_α overlapped by the K K_α peak. Then K K_α and K K_α peaks were stripped from the spectrum to resolve the remaining Ca K_α peak. We also checked the performance of our deconvolution routine by using control enamel specimens.

Z. Skobe: How did Ca retention in the freeze-dried specimens compare with the PPA material?

In Figures 10 and 11, what part of the ameloblast was analyzed? Can these be compared to Figures 13 - 15?
Authors: Control freeze-dried specimens retained more calcium (Figure 15) than did control PPA material (Figure 11). In Figures 10 and 11 the distal surface of the secretory ameloblasts was analyzed. This is the surface which was in contact with enamel prior to separation. Figures 10, 11, 13, 14 and 15 have the same vertical scales, (VS:2500) for peak height. Therefore, they can be compared.

Z. Skobe: Was plasma Ca concentration measured at the time of sacrifice of the Co and F injected rats? If so, was there any decrease in Ca when compared to the control rats?
Authors: Plasma Ca concentration was not measured in any of the animals.

Z. Skobe: Comparison of Figures 10 and 11 indicates that not only was more Ca retained in the PPA material, but also P, S and K, if it is correct to assume that Cl appeared constant between the two groups. Can the authors please comment on this phenomenon?
Authors: When Figures 11 and 12 are compared, chlorine appeared constant between two groups because physiological saline solution was used for cooling during cutting of the mid-sagittal slices of the rat incisor.